powders

MDPI

Article

Hot Consolidation of Titanium Powders

Gennady A. Pribytkov, Irina A. Firsina *, Anton V. Baranovskiy and Vladimir P. Krivopalov

Institute of Strength Physics and Materials Science, Siberian Branch Russian Academy of Sciences, 2/4, pr. Akademicheskii, 634055 Tomsk, Russia; gapribyt@mail.ru (G.A.P.); nigalisha@gmail.com (A.V.B.)
* Correspondence: iris1983@yandex.ru

Abstract: A novel method of the hot consolidation metal powders with shear deformation is proposed. The powders were encapsulated into tight containers and compacted after short-term heating in a furnace preheated to 900 °C. The method prevents powder oxidation, peripheral spalling and ensures the removal of the oxide films from the powder surfaces. Commercial titanium powders of different dispersivities and impurity concentrations were hot-compacted. The microstructure, hardness and bending strength of the compacts were investigated. The compacts from fine PTOM-1 powder, containing 0.32% of hydrogen, reveal the greatest values of the hardness and bending strength. Additional annealing results in 60% increase in the bending strength.

Keywords: titanium powders; hot compaction; annealing; hardness; bending strength

1. Introduction

Products from titanium and its alloys for structural purposes are produced mainly by conventional metallurgical procedures, i.e., melting → hot deformation → machining. The raw material for titanium smelting is titanium sponge or titanium powders, which in turn are obtained from titanium ore (titanium oxides or salts). A variety of physicochemical methods are used to recover titanium from its ore, but only a few of them are used in industry, as only a few of them have economic or technological advantages [1,2].

To further reduce cost, there were attempts to exclude the melting stage from the technology used to produce semi-finished products from titanium. In most cases this can be achieved through the hot deformation of porous billets obtained by cold pressing and following the sintering of titanium powder. There are two often used methods among traditional quasi-static methods for compacting porous billets. In the hot pressing (HP) method, the billet is subjected to uniaxial pressing in a closed mold at a high temperature, and thus the diffusion healing of pores occurs, stimulated by external pressure (i.e., pressure sintering). In another method, i.e., hot isostatic pressing—HIP—the billet, being held at a high temperature under all-round hydrostatic compression, is compacted. Both of these methods require specialized equipment and require that the powder or powder compact are protected from oxidation. However, success is not always guaranteed. In [3], after HIP (960 °C, 140 MPa, 270 min) of porous pre-sintered billets from spongy titanium, densification occurred only on the 1500–1600 μm thick surface layer. The porosity of the underlying part of the billets remained unchanged.

Dynamic methods of compacting titanium powders are used too. For high-speed compaction, various methods are used [4] including hydrodynamic [5,6], magnetic dynamic [7], electric discharge, and explosive. The simplest dynamic loading is realized by dropping a heavy hammer on the porous workpiece. In all cases, either the energy of the moving impactor or the impact velocity serve as measures of the intensity of the impact on the powder. Less common methods of high-speed compaction are also described; for example, the consolidation of the powder by plasma flow, generated during the explosive evaporation of aluminum foil under an electric discharge [8]. At high-speed loading, instant heating of the powder and its plasticization occur. However, due to the short duration of

Citation: Pribytkov, G.A.; Firsina, I.A.; Baranovskiy, A.V.; Krivopalov, V.P. Hot Consolidation of Titanium Powders. *Powders* **2023**, *2*, 484–492. https://doi.org/10.3390/powders2020029

Academic Editor: Paul F. Luckham

Received: 17 March 2023
Revised: 6 June 2023
Accepted: 9 June 2023
Published: 13 June 2023

the thermomechanical action, it is not possible to obtain a completely pore-free material. In most cases, dynamic compaction is used to produce billets for subsequent sintering. The diffusion coalescence of adjacent powder particles occurs resulting in density increase, which ensures the high strength and ductility of the sintered material.

Intensive research aimed at obtaining dense billets by sintering and/or hot stamping of titanium powders began in the 1970s. It was found [9,10] that despite the relatively high melting point (1668 °C), titanium powders are already sintered at 900 °C. To reduce the porosity of sintered billets, they are additionally subjected to hot deformation, usually dynamic stamping. With one-sided pressing in a closed die, the compaction degree and porosity change along the height of the pressing due to friction against the walls of the matrix. To prevent or reduce this inhomogeneity, double-sided pressing [11] or pressing with counterpressure [12] is used. The use of the effect of shear deformation is considered for improving of mechanical properties of hot-pressed powder billets [13,14]. With a lateral relative displacement of the adjacent particles at the shear deformation, oxide films are removed, resulting in the formation of contacts between juvenile surfaces. To extend the shear component of deformation during hot stamping, the molds of a special design with "outflow elements mode" are used [15]. In this case, a density of 99.8–100% is achieved with a pressure of 560–650 MPa, while the density does not exceed 98–98.5% when stamping in a closed die with a pressure of 700–800 MPa [16]. The heating temperature for hot compaction greatly affects density and ductility. Acceptable plasticity appears only after the hot deformation of titanium billets heated at 850 °C and above. Deformation due to the route that provides the shear component gives an additional increase in plasticity.

When porous titanium billets are heated in air for stamping, the oxidation of the surface layer is possible, especially during furnace heating [17]. Therefore, it is necessary to use short-term induction heating or protective atmosphere heating. A proportion of the shear deformation during stamping in a closed die is greater when the diameter of feedstock for compacting is smaller than the diameter of the die matrix. However, with a large difference in these diameters, as well as under free upsetting, cracking of the peripheral regions of the compact can occur due to the strong inhomogeneity of deformation in the radial direction [18]. To prevent this cracking, a constant lateral support of the compacted billets is necessary. This requirement was carried out in our work offering a novel method of the powders' consolidation. In our pressing facility design, presented in Figure 1, a permanent lateral support is provided with a round form of the container filled with the powder. Due to the lateral support, the peripheral cracking of the pressing is prevented. Another advantage of the offered powders' pressing method is a large percentage portion of tangential deformation. Because of relative displacement of the adjacent particles' surface oxide, films are removed from the hot compaction route resulting in the particles welding. More firm jointing of the adjacent particles is expected after vacuum annealing. The practical purpose of the work was to establish the modes of hot compaction (HC) that provide the maximum density and strength of the samples pressed from three titanium powders, which differ in the dispersity and impurity content, and also to study the effect of subsequent annealing on their structure and properties.

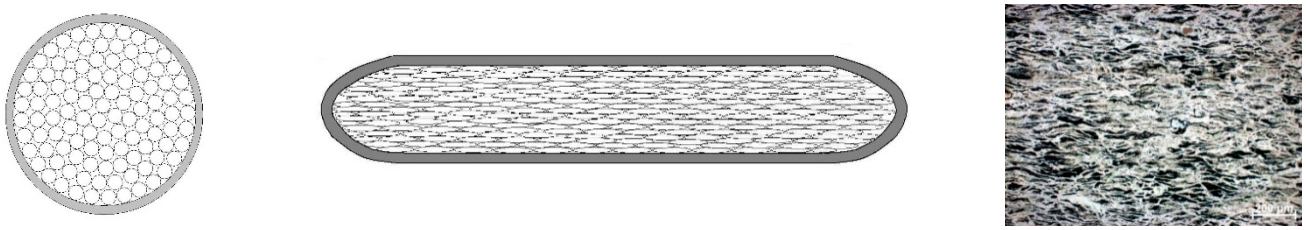

(**a**) (**b**) (**c**)

Figure 1. Schematic image of the container cross sections: (**a**) before hot compaction; (**b**) after hot compaction; (**c**) microstructure in the cross section of the hot-compacted TPP-8 powder.

2. Materials and Experimental Technique

Three types of titanium powders were used, differing in chemical composition and dispersion. The morphology of the powders is illustrated in Figure 2. The data are shown in Table 1.

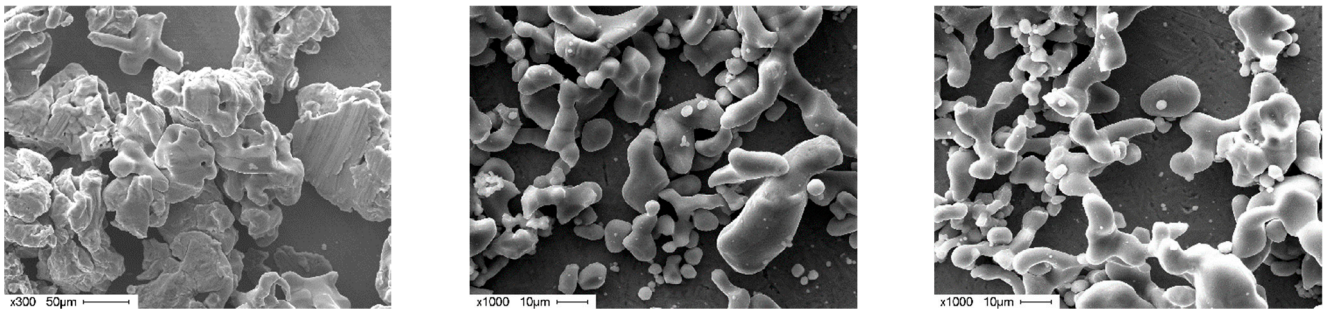

(**a**) (**b**) (**c**)

Figure 2. Morphology of the used powders: (**a**) TPP-8 titanium; (**b**) PTM-1 titanium; (**c**) PTOM-1 titanium.

Table 1. Chemical composition (in wt.%) according to supplier certificates and properties of titanium powders.

Ti Powder	Fe	Ni	Ti	C	Si	Cl	H	N	O	HV_{200}, MPa	Dispersivity, μm
TPP-8	0.29	-	basis	0.05 *	-	0.13	-/0.01 *	0.025/0.006 *	1.04 *	146	<160
PTM-1	0.19	0.20	basis	0.06 *	-	-	0.32/0.29 *	0.07/0.01 *	1.06 *	250	<40 (60%)
PTOM-1	0.18	0.14	basis	0.04 *	0.10	0.003	0.35/0.32 *	0.08/0.01 *	0.97 *	-	<45

The symbol (*) marks the results of chemical analysis.

Powder grade TPP-8 was obtained by sieving a crushed titanium sponge. It is coarser than the other two and differs from them in particle morphology (Figure 2). Another significant difference between PTM-1 and PTOM-1 powders from TPP-8 is a significant hydrogen content (up to 0.35 wt.%). The powders were studied using an X-ray diffraction in Cu Kα irradiation. The phase identification based on the results of the X-ray diffraction, presented in Figure 3, is carried out using the ASTM X-ray database and RENEX and PDWIN software programs. According to the results of the X-ray phase analysis, these powders contain about 5% TiH_2 hydride, which provides a higher microhardness of PTM-1 and PTOM-1 powders, compared to those of the TPP-8 powder.

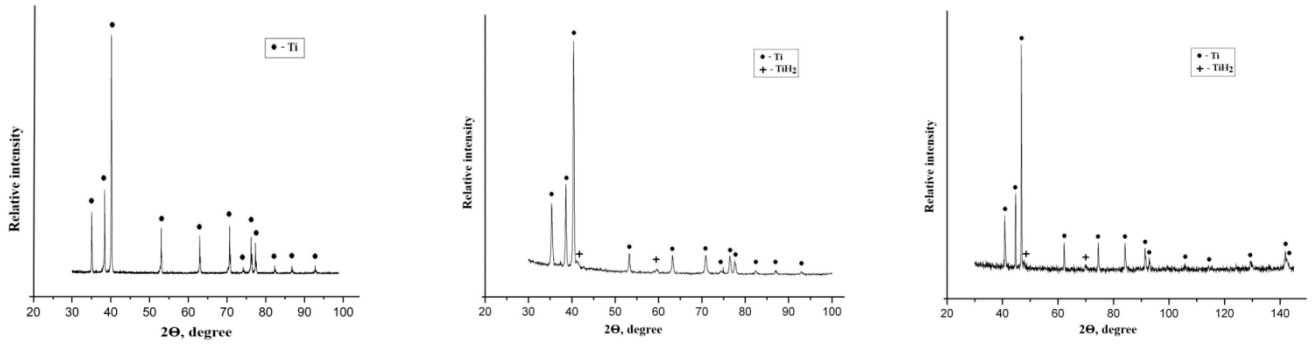

(**a**) (**b**) (**c**)

Figure 3. X-ray diffraction patterns of the used powders: (**a**) TPP-8 titanium; (**b**) PTM-1 titanium; (**c**) PTOM-1 titanium.

Table 1 provides information about the dispersion, hardness and content of the main impurities in the used powders.

Powders obtained from suppliers were additionally analyzed for gas impurities (oxygen, nitrogen, hydrogen) and carbon. A LECO ONH 836 instrument was used for chemical analysis for gas impurities, and an AN-7529M instrument for carbon analysis. According to the results of the analyses, the actual content of hydrogen and carbon corresponded to the suppliers' certificates, and the nitrogen content turned out to be an order of magnitude lower than the threshold values of the certificates. The oxygen content in the powders was about 1 wt.%.

For hot compaction in the quasi-static mode, the powders were encapsulated into air-tight containers made from a thin-walled steel tube with an outer diameter of 14 mm. The containers were put in a furnace, preheated to 900 °C, held for 15 min, and pressed and kept under pressure for 10 s. The heating temperature of the containers and the pressing force were chosen by taking into account known data on hot stamping on titanium. To prevent rapid cooling during pressing, heat-insulating 0.8 mm thick asbestos spacers were placed between the press plate and container. After cooling, the pressed powder sheets were extracted from the steel shell. The size of the sheets in the cross section was $(2.6 \pm 0.2) \times (21 \pm 1.0)$ mm, depending on the grade of titanium powder and the hot compacting pressure. The density of the sheets pressed under different pressures was determined by Archimedes' principle method. Some of the hot-compacted sheets were annealed in 10^{-2} Pa vacuum at 870 °C for 2 h and at 1300 °C for 1 h.

Samples that were 2.5 × 10 × 32 mm in size for bending tests, samples for X-ray diffraction analysis and for metallographic investigation were cut from the sheets obtained at maximum pressure. Metallographic sections were prepared by grinding and polishing using diamond pastes. The sections were etched with Keller's reagent (2.5 mL HNO_3 + 1.0 mL HF (45%) + 1.5 mL HCl + 95 mL H_2O). INSTRON 1185 testing machine was used for three-point bending tests according to GOST 57749-2017 at a loading speed of 0.5 mm/min. Flexural strength σ_f (MPa) was calculated using formula $\sigma_f = \frac{3F_mL}{2bh^2}$, where F_m is the maximum load, H; L is the distance between lower supports, mm; b is the sample width, mm; h is the sample thickness, mm. Elastic modulus E (GPa) was calculated using the formula $E = \frac{FL^3}{48\Delta I_z}$, where F is the load, N; L is the distance between lower supports, m; Δ is the advance of the upper traverse of the testing machine, m; $I_z = \frac{bh^3}{12}$ is the axial moment of the inertia of the piece; b is the sample width, m; h is the sample thickness, m. The ratio $\frac{F}{\Delta}$ was taken from the linear area of the loading plot.

3. Results and Discussion

3.1. Structure of the Consolidated Powders

Reasonable dependences of density and residual porosity on the pressing pressure were obtained in the hot compaction of the TPP-8 powder. The porosity of the compacts decreases together with the density rise when the pressure increases. High-temperature (1300 °C) annealing of hot-compacted samples results in further increase in density and reduction in porosity (Figure 4).

A similar monotonic dependence of density on pressure was also obtained for PTM-1 powder, while for PTOM-1 the density did not change within the scatter. The different behavior of the density of PTM-1 and PTOM-1 powders during hot compaction is evidently explained by their different dispersity and the effect of hydrogen impurities in the powders. The dependence of the powders' compacting ability on the particles' size is well known. Hydrogen content in PTM-1 and PTOM-1 powders does not differ much (0.29 and 0.32%, respectively), but the hydrogen content difference can increase during heating before compaction due to a higher rate of the hydrogen escaping from finer PTOM-1 powder. The two aforesaid reasons, in our opinion, can result in the density difference of the compacted powders. However, after high-temperature annealing, the density of compacts from PTM-1 and PTOM-1 also increased in a similar fashion to that of TPP-8. The highest density was obtained for annealed samples compacted at maximum pressure. The porosity of compacts from the PTM-1 and PTOM-1 powders was not calculated, since it was considered incorrect

to use the reference values for pure titanium as theoretical density for the powders with hydrogen impurity.

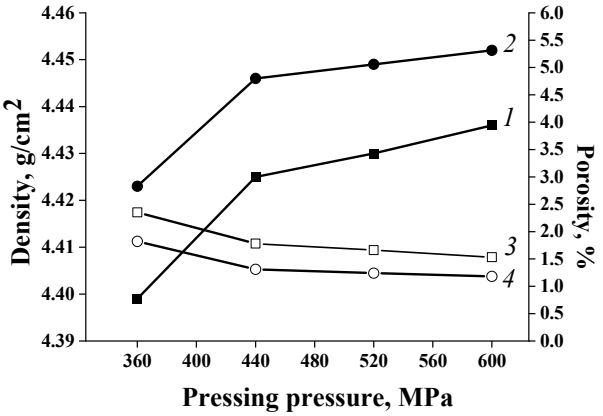

Figure 4. Dependence of the density (1,2) and porosity (3,4) of TPP-8 hot-compacted powder on the pressure of hot compaction: 1,3—after hot compaction; 2,4—after hot compaction followed by annealing at 1300 °C, 1 h.

Figure 5 shows optical images of the microstructure of hot-compacted TPP-8 and PTOM-1 powders, which differ significantly in dispersion and hydrogen content. The microstructures, after additional annealing at 870 °C, are also shown. The annealing temperature was chosen to be below $\alpha \rightarrow \beta$ allotropic transformation (882 °C) in order to exclude its effect on the microstructure.

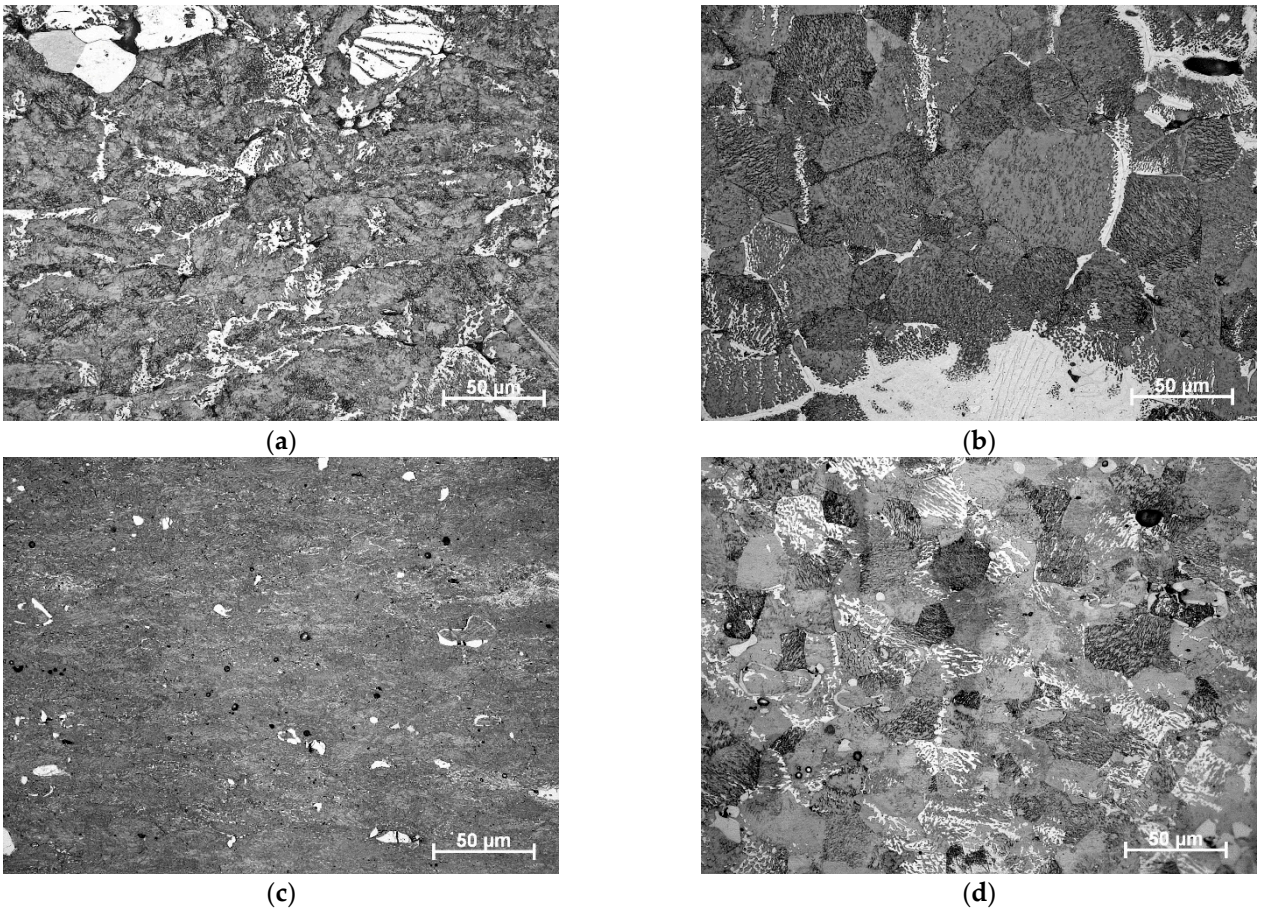

(**a**) (**b**) (**c**) (**d**)

Figure 5. Microstructure of hot-compacted compacts from TPP-8 (**a**,**b**) and PTOM-1 (**c**,**d**) powders, (**a**,**c**) after hot compaction, (**b**,**d**) after hot compaction followed by annealing at 870 °C, 2 h.

Different dispersities of the powders and hydrogen in the PTOM-1 powder are the reasons for the difference in the compacts' microstructure. On the sections of compacts from TPP-8, grains with etched boundaries are elongated perpendicular to the pressing direction. On the sections of the PTOM-1 powder compacts, grain orientation is also perpendicular to the pressing direction; however, the structure is finer and the grain boundaries are barely distinguishable (Figure 5a,c). After annealing, recrystallization occurs. The size of recrystallized grains in PTOM-1 is approximately three times smaller than the size of grains in TPP-8 (Figure 5b,d).

3.2. Mechanical Properties and Fracture Features of the Consolidated Powders

Table 2 shows the results of determining the microhardness and bending tests of hot-compacted powders before and after annealing at 870 °C for 2 h. The microhardness of PTOM-1 plates is, on average, 70% higher than that of TPP-8 plates, which can be explained by the fact that TPP-8 powder is less hard compared to hydrogen—containing powders (see Table 1). The additional contribution to PTOM-1 hardness renders the finer grain structure of PTOM-1. The assumption about the strengthening effect of hydrogen in PTOM-1 is confirmed by the fact that the hardness decreases after vacuum annealing due to the release of hydrogen dissolved in titanium. According to reference data [19], the release of hydrogen from titanium powder upon heating in vacuum begins at 550 °C. However, it is possible that a two-hour holding at 870 °C is not enough for hydrogen to escape from the plates. The remaining hydrogen provides relatively high hardness. In contrast to PTOM-1, the hardness of TPP-8 plates increases slightly during annealing.

Table 2. Mechanical properties of hot-compacted titanium powders.

Ti Powder	Processing	HV_{200}, MPa	*E*, GPa	σ_f, MPa
TPP-8	HC	2079 ± 210	39 ± 4	509 ± 23
	HC+annealing 870 °C, 2 h	2174 ± 195	47 ± 2	712 ± 25
PTOM-1	HC	3688 ± 220	55 ± 2	723 ± 20
	HC+annealing 870 °C, 2 h	3288 ± 206	64 ± 2	1148 ± 55

The bending strength and elastic modulus of TPP-8 compacts are lower than those of PTOM-1 compacts. Additional annealing at 870 °C increases the strength and elastic modulus. The greatest effect of annealing on strength is shown in the PTOM-1 hot-compacted samples. The elastic modulus increases by 15–17% during annealing. However, the values calculated from the "F − Δ" curves are half of the reference data for pure titanium (110 GPa), and therefore, cannot be considered reliable. The reason for this difference may be, on the one hand, the complex stress—strain state of the material under three-point bending. On the other hand, the value of Δ does not reflect the true deformation of the material, perhaps due to the elastic deformation and collapse of the samples in contact areas with the supports and the deforming roller. More accurate values of the elastic modulus of various materials (steel, graphite) under three-point bending were obtained [20], using the method of digital image correlation (laser speckle pattern interferometry). In this method, the true deformation is determined by the displacement of points on the plate's surface.

According to the view of the typical diagrams (Figure 6) and patterns of fracture surfaces (Figure 7), the destruction of TPP-8 compacts is preceded by plastic deformation, the value of which is especially large on annealed samples. The powder particles are tightly pressed to each other during hot compaction (Figure 7a). The diffusion coalescence of adjacent powder particles occurs during annealing (Figure 7b). The diffusion coalescence of adjacent grains begins during exposure under pressure during hot compaction, but due to the short duration of the exposure (10 s) and the decrease in temperature due to heat removal, its effect on strength and ductility is insignificant.

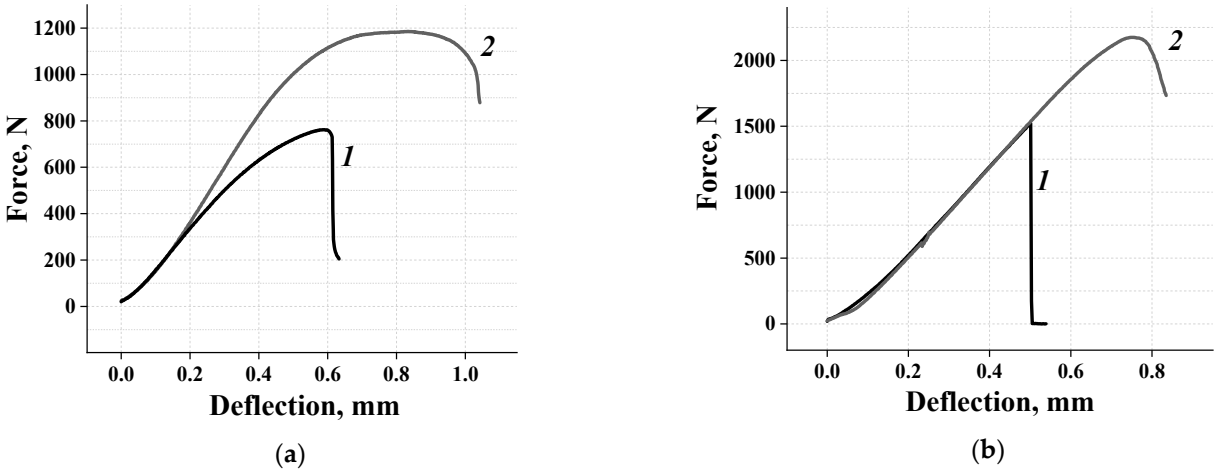

Figure 6. "Force–deflection" diagrams during bending tests of the hot-compacted billets from TPP-8 (**a**) and PTOM-1 (**b**) titanium powders: 1—after hot compaction; 2—after hot compaction followed by annealing at 870 °C, 2 h.

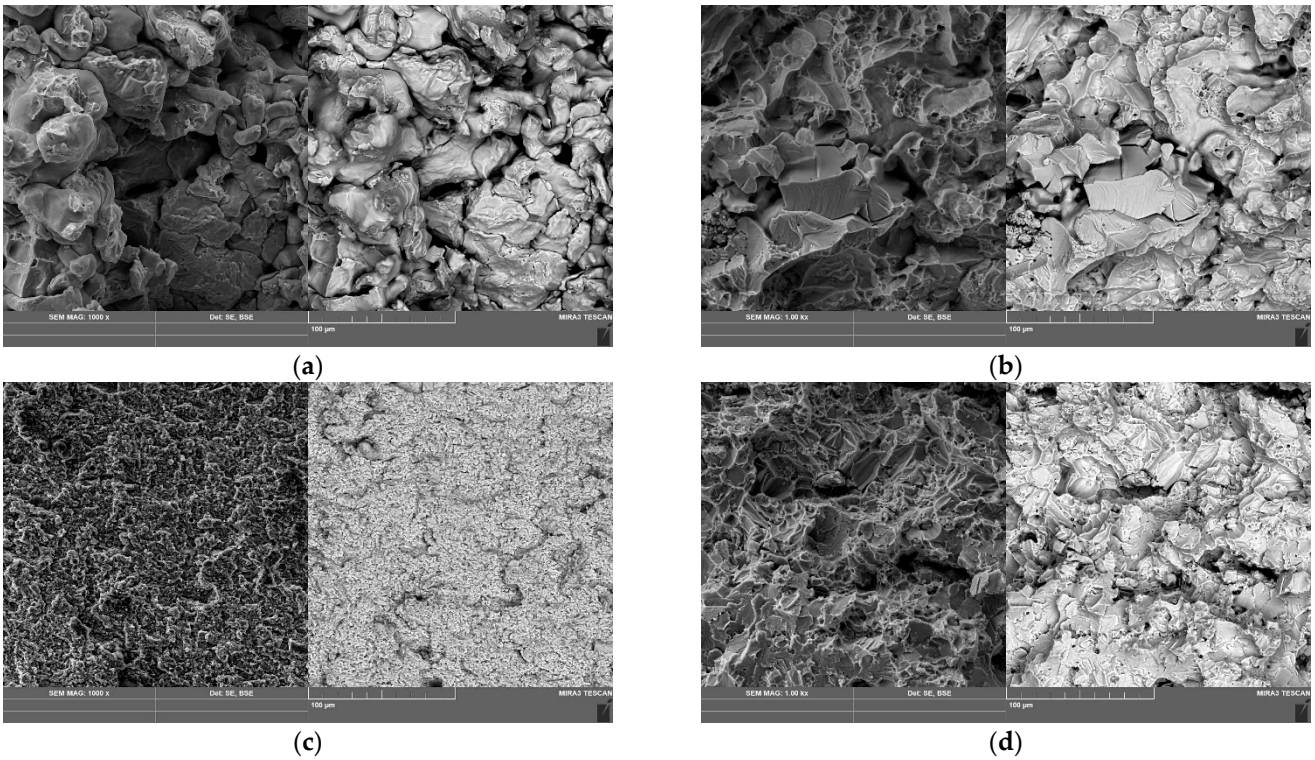

Figure 7. Fracture surfaces during bending tests of the hot-compacted billets from TPP-8 (**a**,**b**) and PTOM-1 (**c**,**d**) titanium powders: (**a**,**c**) after hot compaction; (**b**,**d**) after hot compaction and annealing at 870 °C, 2 h. Left side—secondary electron image (SE); right side—back-scattered electron image (BSE).

The fracture of PTOM-1 hot-packed compacts is brittle, as shown in Figure 6b, and the bending strength is relatively low. However, after annealing, the strength increases. Curve 2 in Figure 6b shows a plastic deformation region that precedes fracture. On the fracture surface, as presented in Figure 7d, regions of ductile fracture are visible. This becomes possible due to the diffusion coalescence of the adjacent Ti particles.

The bending strength of the PTOM-1annealed compacts is 60% higher than that of the TPP-8 annealed compacts. One of the reasons for this, in our opinion, is the greater dispersivity of the PTOM-1 powder. This explains the greater specific surface area of

adjacent boundaries in the hot-packed billets, on which diffusion coalescence occurs during annealing. It is also possible that hydrogen, which is present in the PTOM-1 powder and partially remains in the compact after vacuum annealing, exerts a positive influence on the strength. The mechanisms of the positive effect of hydrogen can also be the purification of the material from oxygen dissolved in titanium and diffusion acceleration in the process of diffusion coalescence.

4. Conclusions

1. A method of hot compaction of titanium powders using shear deformation is proposed. The method promotes the removal of oxide films from the surfaces of adjacent particles, prevents peripheral cracking and provides residual porosity by not more than 1.0–1.5%;
2. The hardness and bending strength of the resulting compacts depend on the dispersivity and hydrogen content of the titanium powder. The highest values of hardness and bending strength have compacts pressed from fine PTOM-1 grade titanium powder, which contains 0.32% hydrogen. The annealing of PTOM-1 compacts at a temperature below $\alpha \rightarrow \beta$ transformation temperature increases the bending strength by 60% and moves the fracture from brittle area to brittle—ductile area.

Author Contributions: Conceptualization, G.A.P.; methodology G.A.P.; writing—original draft preparation, G.A.P.; validation—V.P.K.; investigation—I.A.F. and A.V.B.; formal analysis—I.A.F. and A.V.B.; writing—review, editing and translation—I.A.F.; data curation—A.V.B.; visualization—I.A.F. and A.V.B.; supervision, G.A.P.; project administration, G.A.P.; resources—G.A.P. and V.P.K. All authors have read and agreed to the published version of the manuscript.

Funding: The work was carried out within the framework of the state task of the ISPMS SB RAS, project number FWRW-2021-0005.

Institutional Review Board Statement: Not applicable.

Informed Consent Statement: Not applicable.

Data Availability Statement: The data presented in this study are available on request from the corresponding author. The data are not publicly available due to privacy.

Conflicts of Interest: The authors declare no conflict of interest.

Abbreviations

The following abbreviations are used in this manuscript:

HP	hot pressing.
HIP	hot isostatic pressing.
HC	hot compaction.
SE	secondary electron image.
BSE	back-scattered electron image.

References

1. Crowley, G. How to extract low-cost titanium. *Adv. Mater. Process.* **2003**, *161*, 25–27.
2. Froes, F.H.S.; Gungor, M.N.; Imam, M.A. Cost-affordable titanium: The component fabrication perspective. *JOM* **2007**, *59*, 28–31. [CrossRef]
3. Pavlenko, D.V. Technological methods of sealing sintered titanium billets. [Tekhnologicheskiye metody uplotneniya spechennykh titanovykh zagotovok]. *Her. Aeroenginebuild. [Vestnik Dvigatelestroeniya]* **2015**, *1*, 87–93. (In Russian)
4. Sethi, G.; Myers, N.S.; German, R.M. An overview of dynamic compaction in powder metallurgy. *Int. Mater. Rev.* **2008**, *53*, 219–234. [CrossRef]
5. Yan, Z.; Chen, F.; Cai, Y. High-velocity compaction of titanium powder and process characterization. *Powder Technol.* **2011**, *208*, 596–599. [CrossRef]
6. Yan, Z.; Chen, F.; Cai, Y.; Yin, J. Influence of particle size on property of Ti−6Al−4V alloy prepared by high-velocity compaction. *T. Nonferr. Metal. SOC* **2013**, *23*, 361–365. [CrossRef]
7. Dong, D.; Huang, X.; Cui, J.; Li, G.; Jiang, H. Effect of aspect ratio on the compaction characteristics and micromorphology of copper powders by magnetic pulse compaction. *Adv. Powder Technol.* **2020**, *31*, 4354–4364. [CrossRef]

8. Vivek, A.; Defouw, J.D.; Daehn, G.S. Dynamic compaction of titanium powder by vaporizing foil actuator assisted shearing. *Powder Technol.* **2014**, *254*, 181–186. [CrossRef]
9. Arensburger, D.S. Sinter ability of titanium powder. *Powder Metall. Met. Ceram.* **1970**, *9*, 113–116. [CrossRef]
10. Arensburger, D.S.; Pugin, B.C.; Fedorchenko, I.M. Properties of electrolytic and reduced titanium powders and sinter ability of porous compacts from such powders. *Powder Metall. Met. Ceram.* **1968**, *7*, 362–367. [CrossRef]
11. Bagliuk, G.A.; Stern, M.B.; Yurchuk, V.L. A comparative analysis of loading modes in the hot re-pressing of a porous blank in a closed die. *Powder Metall. Met. Ceram.* **1989**, *28*, 845–847. [CrossRef]
12. Sypko, A.V.; Dolgii, N.I.; Gavrilov-Kryamichev, N.L. Dynamic forging of parts from titanium powder with counter pressure. *Powder Metall. Met. Ceram.* **1978**, *17*, 567–569. [CrossRef]
13. Bagliuk, G.A. Technological problems of the processes of hot stamping porous blanks [Tekhnologicheskiye problemy protsessov goryachey shtampovki poristykh zagotovok]. *J. Mech. Eng. NTUU "Kyiv Polytech. Ins. [Vísnik Natsíonal'nogo Tekhníchnogo Unívesitetu Ukraîni «Kîvs'kiy Polítekhníchniy Institut». Seriya: Mashynobuduvannya* **2009**, *56*, 93–100. (In Russian)
14. Bagliuk, G.A. Influence of deformation parameters on the structure and properties of hot-forged powder materials [Vliyaniye deformatsionnykh parametrov na strukturu i svoystva goryacheshtampovannykh poroshkovykh materialov]. *Press. Mat. Process. [Obrabotka Materialov Davleniyem]* **2011**, *26*, 139–145. (In Russian)
15. Obodovskii, E.S.; Laptev, A.M. Effect of technological factors on the properties of high-density titanium sponge compacts. *Powder Metall. Met. Ceram.* **1987**, *26*, 295–299. [CrossRef]
16. Pavlov, V.A.; Nosenko, M.I.; Karlov, L.A. Thermomechanical regime of hot forgine of titanium powder preform. *Powder Metall. Met. Ceram.* **1991**, *30*, 899–903. [CrossRef]
17. Rakovskii, V.S.; Borzetsovskaya, K.M.; Olenina, N.S.; Bolotina, T.A. Hot deformation of sintered titanium powder preforms. *Powder Metall. Met. Ceram.* **1973**, *12*, 71–74. [CrossRef]
18. Lyashenko, A.P.; Pavlov, V.A.; Boguslaev, V.A.; Karlov, L.A.; Avrunina, G.V. Production of P/M titanium materials by hot forging. *Powder Metall. Met. Ceram.* **1984**, *12*, 85–854. [CrossRef]
19. Dorofeev, G.A.; Lad'yanov, V.I.; Lubnin, A.N.; Mukhgalin, V.V.; Kanunnikova, O.M.; Mikhailova, S.S.; Aksenova, V.V. Mechanochemical interaction of titanium powder with organic liquids. *Int. J. Hydrogen Energy* **2014**, *39*, 9690–9699. [CrossRef]
20. Goltsev, V.Y.; Osintsev, A.V.; Plotnikov, A.S. Determination of the material elasticity modulus in bending. *Lett. Mater.* **2017**, *2*, 91–95. [CrossRef]